Lipids in Health and Disease

RESEARCH

Open Access

SRT3025-loaded cell membrane hybrid liposomes (3025@ML) enhanced anti-tumor activity of Oxaliplatin via inhibiting pyruvate kinase M2 and fatty acid synthase

Xiaobin Wang[1*], Shulin Li[1], Zichen Li[2], Zhuona Lin[3] and Zhifeng Wang[4*]

Abstract

Background Bladder cancer is one of the most common malignancies of the urinary system. Despite significant advances in diagnosis and treatment, the compromised therapeutic effect of chemotherapeutic agents, such as Oxaliplatin (OXA), remains a major clinical challenge. Thus, a combination therapy is required to enhance the OXA's therapeutic effectiveness and improve patient outcomes.

Methods The thin film hydration method was used to prepare the liposomes. Drug encapsulation efficiency and loading capacity were determined to investigate the advantages of the SRT3025-loaded cell membrane hybrid liposomes (3025@ML). Bladder cancer cell lines T24 and 5637 were cultured in McCoy's 5 A and RPMI 1640 medium, respectively. The Cell Counting Kit-8 assay was used to determine the cell viability by treating cells with a medium containing either the vehicle solution (control), the cell membrane hybrid liposomes (ML), 3025@ML, or compound 3 K. The antiproliferative activities were investigated after treating cells with OXA + 3025@ML and compound 3 K + OXA. Cell death and apoptosis were quantified by trypan blue and Annexin V-APC/PI apoptosis assay after treating cells with control, OXA, OXA + 3025@ML, and 3025@ML. Western blot analysis was performed after treating cells with 3025@ML, OXA, 3 K, 3025@ML + OXA, and 3 K + OXA to determine the protein levels of pyruvate kinase M2 (PKM2) and fatty acid synthase (FASN), etc.

Results The present study demonstrated that 3025@ML enhances the chemotherapeutic effect of OXA. 3025@ML + OXA treated T24 and 5637 cells showed that combination therapy significantly reduced cell viability and increased cell death rate. Flow cytometry analysis showed that the combination of 3025@ML and OXA significantly increased the percentage of apoptotic cells in T24 cells. 3025@ML and compound 3 K reduced the levels of FASN in T24 and 5637 cells and increased the anti-tumor activity of OXA. Mechanistic studies showed that 3025@ML inhibited the PI3K/AKT/mTOR signaling pathway and reduced the expression of key metabolic regulators PKM2 and FASN.

*Correspondence:
Xiaobin Wang
wxb6890286@163.com
Zhifeng Wang
wzfshengyi@zzu.edu.cn

Full list of author information is available at the end of the article

Furthermore, this study demonstrated that targeting lipid metabolism and inhibiting FASN can effectively overcome the compromised therapeutic effect of OXA.

Conclusion The study demonstrated that 3025@ML significantly enhances the anti-tumor activity of OXA. This novel drug delivery system inhibits key metabolic pathways, which increase DNA damage and tumor cell apoptosis. The results indicate that 3025@ML is a promising therapeutic strategy for overcoming OXA's compromised therapeutic effect and potentially improving cancer treatment outcomes.

Keywords Bladder cancer, SRT3025, Oxaliplatin, PKM2, FASN

Introduction

Bladder cancer is the most prevalent tumor of the urinary system [1]. Although surgical resection considerably prolongs the patient's survival, a subset of individuals still experiences tumor recurrence within 5 years [2, 3]. Therefore, chemotherapy remains the most common treatment option for patients with unresectable tumors. Oxaliplatin (OXA) is the most commonly used chemotherapeutic agent for tumor treatment. However, several factors contribute considerably to the suboptimal treatment outcomes of OXA, e.g., enhanced drug efflux, DNA repair, and metabolic reprogramming, etc [4, 5]. Thus, combination therapy of OXA is urgently required to improve the efficacy of OXA-based therapies. OXA, as a third-generation platinum, enters tumor cells and binds to DNA, forming a hairpin-like structure that leads to DNA damage and subsequently induces cell death. Notably, targeting the tumor cells' metabolic pathways without eliciting toxicity to normal cells has been identified as a promising approach for treating cancer [6, 7]. Inhibition of the activity of pyruvate kinase M2 (PKM2), an isoform of pyruvate kinase, a crucial regulator of cellular energy metabolism, enhances the anti-tumor activity of chemotherapy [8, 9].

Fatty acid synthase (FASN) is a multifunctional enzyme crucial in synthesizing long-chain saturated fatty acids, particularly palmitic acid, within cells. The FASN plays an essential role in cellular lipid metabolism by providing fatty acids necessary for several vital processes, such as cell membrane synthesis, energy storage, and synthesis of signaling molecules. Recent studies proved that FASN regulated PKM2 and induced chemoresistance [10–12]. PKM2 and FASN contribute to OXA resistance by altering metabolism and boosting lipid production, respectively [13].

Sirtuin (SIRT1)-activating compounds (STACs) are chemical compounds, such as SRT2183, SRT3025, and SRT1720, that influence the activity of sirtuins, a class of enzymes that utilize NAD^+ to deacetylate proteins. SRT3025, a water-insoluble compound, has shown excellent anti-tumor effects [14]. Treatment with the SIRT1 activator SRT2104 attenuated inflammatory damage, promoted autophagy, and decreased the levels of PKM2 [15].

SRT3025 is well tolerated in mice and can potentially be employed in treating various diseases [14]. However, no study has reported the relationship between SRT3025 and PKM2. Additionally, it is reported that nanomedicines offer significant advantages in tumor treatment by protecting the drugs, enhancing their solubility, accumulation, and penetration within tumor tissues, and minimizing adverse reactions to normal tissues [16]. These benefits emphasize the promising future of nanomedicines in oncology.

Cell membrane hybrid liposome (ML) is an innovative nanocarrier combining natural cell membranes' advantages with synthetic liposome's structural benefits [17]. Compared to the traditional liposome, ML is covered by cell membranes, which helps the nanoparticle evade surveillance and elimination by the immune system. T24 cells from human bladder metastatic cell carcinoma have a membrane composition well-suited for targeting bladder cancer. Coating nanocarrier with T24 membranes enhances binding and uptake by these cancer cells, enabling efficient targeting while protecting healthy cells and decreasing the side effects of therapies. The novelty of this study lies in its innovative strategy for cancer treatment using cell membrane hybrid liposomes containing SRT3025 and combination therapy with OXA. This study aims to evaluate the synergistic effect of SRT3025-loaded cell membrane hybrid liposomes (3025@ML) combined with OXA and to understand the key metabolic pathways involved, which provides new perspectives for improving the treatment of bladder cancer.

Methods

Cell culture and reagents

The bladder cell lines T24 cells and 5637 cells were purchased from Stem Cell Bank (Chinese Academy of Sciences, Beijing, China) and cultured in McCoy's 5 A medium (Thermo Fisher Scientific, Waltham, MA, USA, catalog no. 16600082) or RPMI 1640 medium (Thermo Fisher Scientific, Waltham, USA catalog no. 11875093) with 10% fetal bovine serum (FBS, AusGeneX, Gold Coast, Australia, catalog no. FBS500-S). Oxaliplatin (OXA, catalog no. S1224), SRT3025 (catalog no. S8481), and compound 3 K, the inhibitor of PKM2, (3 K, catalog

no. S8616), were purchased from Selleck Chemicals (Houston, USA).

Synthesis of the 3025@ML

To synthesize SRT3025-loaded cell membrane hybrid liposomes (3025@ML), a mixture of 1,2-Dimyristoyl-sn-glycero-3-phosphocholine (DMPC, Avantor Inc., Radnor, PA, USA, catalog no. S01003), 1,2-Dipalmitoyl-sn-glycero-3-phosphocholine (DPPC, Avantor Inc., catalog no. S01004), and 1,2-Distearoyl-sn-glycero-3-phosphoethanolamine-N-[methoxy(polyethyleneglycol)2000] (DSPE-PEG2000, Avantor Inc., catalog no. F01008) in a 4:15:1 (n/n/n) ratio was used. SRT3025 was dissolved in chloroform and methanol mixture (9:1, v/v) and vortexed. The organic solvent was then evaporated under reduced pressure using a rotary evaporator at 37 °C and 30 rpm. Once lipid film was formed on the flask's bottom, 1 mL of PBS was added to create a biphasic system, which was then further processed on the rotary evaporator at 45 °C and 60 rpm for 30 min. The resulting suspension was put in an ice bath and sonicated for 2 min to produce 3025@L.

Cell membrane vesicles were harvested and extracted from T24 cells, as reported by Zhang et al. 's method [18]. These vesicles were incubated with 3025@L at 37°C for 15 minutes and then ultrasonicated on ice for 3 minutes to completely fuse the liposome (Lipo) and tumor membrane (Mem), forming 3025@ML. Fluorescently labeled liposomes (Dio-Lipo) and tumor membranes (Dil-Mem) were prepared like 3025@ML, incorporating the dyes 3,3'-Dioctadecyloxacarbocyanine perchlorate (Dio) and 1,1'-Dioctadecyl – 3,3,3',3'-tetramethylindocarbocyanine perchlorate (Dil) for experimental tracking. Figure 1 illustrates the study's workflow and experimental elements.

Characterization of the 3025@ML

To evaluate the stability of nanoparticles, the size distribution and zeta potential of the nanoparticles were determined by Zetatronix 919 (Opptronix, Shanghai, China). To verify the successful formation of the cell membrane hybrid liposomes (ML), Mem and Lipo were labeled with Dil and Dio dyes. Dio-Lipo and Dil-Mem were evaluated by co-localization analysis via an Axio Vert. A1 fluorescence microscope (Carl Zeiss, Oberkochen, Germany). In addition, Lipo, Mem, and ML were added to the SDS gel loading buffer for lysis and boiling. Subsequently, gels were stained with Coomassie brilliant blue to observe membrane protein expression. To examine the cytotoxicity of nanoparticles, 4×10^3 T24 and 5637 cells were seeded per well in a 96-well plate separately and cultured for 24 h. The cells were treated with 0, 1, 10, 100, and 1000 μg/mL of ML for 48 h. CCK8 assay was used to detect the cytotoxicity of ML.

Drug loading capacity and encapsulation efficiency

SRT3025 (1 mg/mL) was dissolved in methanol. The maximum absorption wavelength of SRT3025 was determined using ultraviolet-visible (UV-Vis) scanning spectroscopy. Various ratios of 3025@ML from 1:1 to 1:20 (w/w) (SRT3025:ML) were synthesized to determine the drug loading capacity. Drug Loading Capacity (DLC) and encapsulation efficiency (EE) were calculated using the following formulas:

$$DLC(\%) = \frac{\text{mass of SRT3025 in 3025@ML}}{\text{mass of total SRT3025} + \text{mass of ML}} \times 100\%$$

$$EE(\%) = \frac{\text{mass of SRT3025 in 3025@ML}}{\text{mass of total SRT3025}} \times 100\%$$

Evaluating cellular uptake of 3025@ML

To evaluate the cellular uptake ability of 3025@ML, 2.5×10^5 T24 cells per well were allowed to grow in a 6-well plate for 48 h and incubated with PBS (as a control), 3025@ML and 3025@ML combination with filipin (inhibitors of caveolin-1) at 37 °C and 3025@ML at 4 °C. Following incubation with the respective treatments for 2 h, the cells were washed with cold PBS to remove excess particles. The cells were then trypsinized to detach from the culture plates, collected by centrifugation, and resuspended in cold PBS. Samples were immediately analyzed using flow cytometry to measure the fluorescence intensity of DiI, which corresponded to the amount of 3025@ML internalized by the cells.

Evaluating cell viability

T24 and 5637 cells were seeded at a density of 2.0×10^3 cells per well in a 96-well plate. After 24 h of incubation to investigate the concentration of 3025@ML and 3 K that has an anti-tumor effect, the cells were treated with a medium containing either varying concentrations (0.1, 1, 10, 100 μM) of 3025@ML or 3 K for 48 h. To assess the impact of 3025@ML and 3 K on OXA, cells were plated following the previously described method and subjected to treatment with the control, 3025@ML, 3 K, OXA, 3025@ML + OXA, and 3 K + OXA. Cell viability was evaluated using the Cell Counting Kit-8 (CCK8, MedChemExpress, Monmouth Junction, USA, code HY-K0301). The intensity of the color change was quantified by measuring the absorbance at 450 nm using a Synergy LX multimode reader (BioTek, Winooski, USA).

$$\text{Cell viability } (\%) = \frac{OD \text{ of treated cells}}{\text{OD of control cells}} \times 100\%$$

Evaluating cell death and apoptosis

To evaluate cell death, T24 and 5637 cells were seeded at a density of 3.0×10^4 cells per well in a 24-well plate for

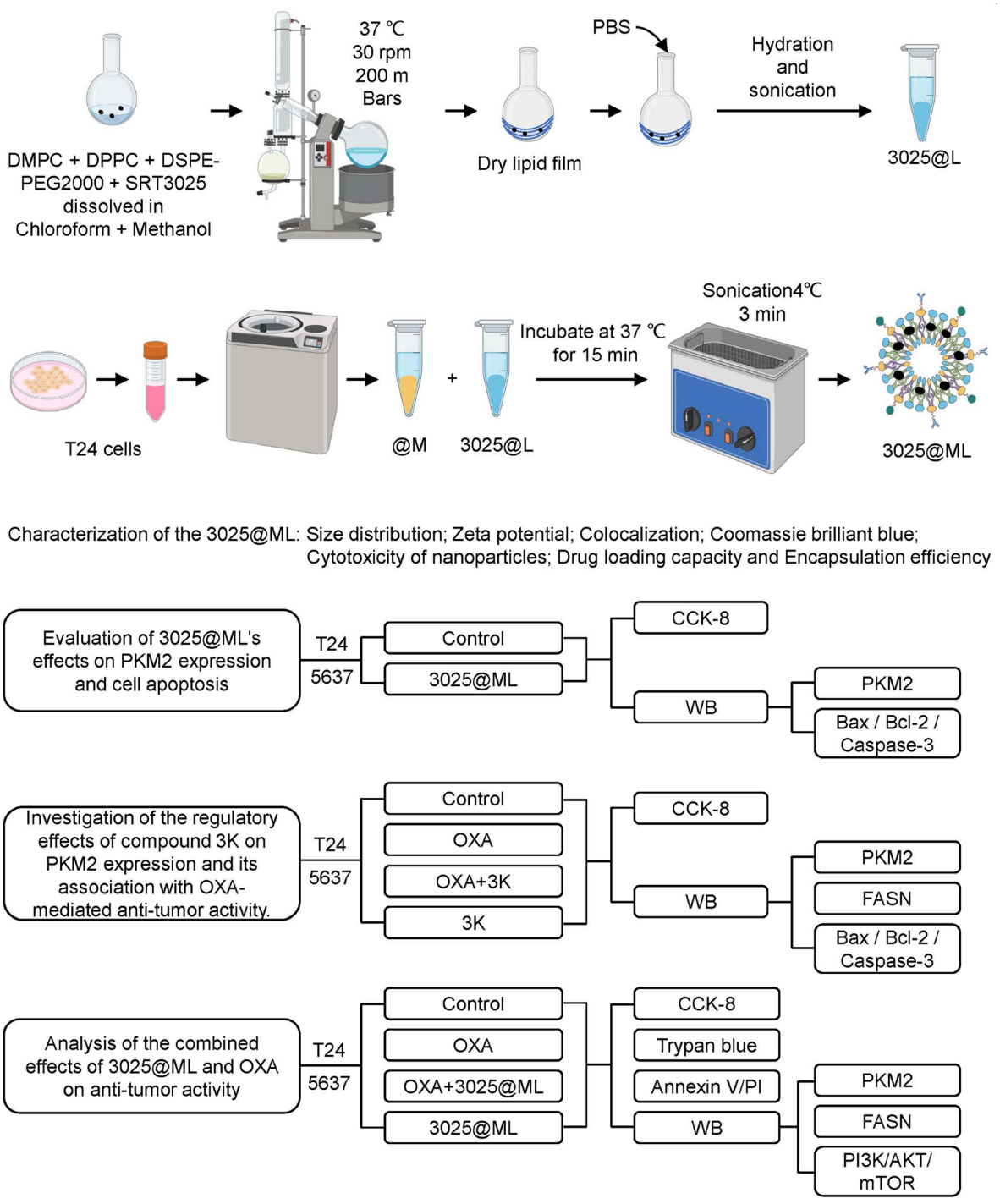

Fig. 1 Experimental design flowchart

24 h. Subsequently, these cells were treated with control, OXA, 3025@ML + OXA, and 3025@ML alone for 48 h. Cell death was quantified by trypan blue staining. For apoptosis analysis, T24 cells were seeded at a density of 2.5×10^5 cells per well in a 6-well plate and treated with control, 3025@ML, OXA, or a combination of both drugs for 48 h. Apoptotic cells were quantified using the Annexin V-APC/PI apoptosis kit (Elabscience, Houston, USA, catalog no. E-CK-A217) and a NovoCyte flow cytometer system (Agilent, Santa Clara, USA).

Evaluating molecular mechanisms

Western blotting (WB) was performed to determine the level of pyruvate kinase M2 (PKM2), fatty acid synthase

(FASN), and the regulation of apoptosis protein, such as BCL2-Associated X protein (Bax), B-cell lymphoma-2 (Bcl-2) and cleaved caspase-3. 2.5×10^5 T24 and 5637 cells were seeded separately per well in a 6-well plate and cultured for 24 h. These cells were treated with the 3025@ML, 3025@ML + OXA, OXA, 3 K, and 3 K + OXA for 48 h. After lysis with RIPA buffer, samples were centrifuged at 10,000× g for 30 min at 4 °C. The supernatant was collected, and the protein concentration was determined. Then, the proteins were denatured by boiling in an SDS-gel loading buffer for 10 min. Equal amounts of protein were subjected to 15% SDS-PAGE. Proteins were blotted onto PVDF Western blot membranes (Roche Diagnostics, Mannheim, Germany) and incubated with antibodies (Table 1). Inhibitors of caveolin-1 (filipin), alongside Dil-labeled 3025@ML, were investigated to evaluate the uptake mechanism of these hybrid liposomes in bladder cancer cells via flow cytometry.

The proteins were visualized with horseradish peroxidase-conjugated goat anti-rabbit IgG (Cell Signaling, Danvers, USA, catalog no. 7074) by using a Thermo Scientific SuperSignal West Femto Maximum Sensitivity Substrate (Waltham, USA, catalog no. 34096).

Gene expression evaluation

In order to investigate changes in gene expression profiles, T24 cells per well were seeded in 6 well plates for 48 h and treated by control and 3025@ML for another 24 h. RNA was extracted with TRIzol (Thermo Fisher Scientific, catalog no. 15596026), and mRNA expression was analyzed using Illumina next-generation sequencing. Differential expressions were assessed with the DESeq2 package in R. Additionally, Gene Ontology (GO) and Kyoto Encyclopedia of Genes and Genomes (KEGG) pathway analyses were conducted to further explore the functional implications of the differentially expressed genes.

Table 1 The following antibodies were used

Antibody	Company	Catalog no.	Dilution
Anti Pyruvate kinase M2 (PKM2)	Cell Signaling Technology, Danvers, MA, USA	4053	1000 ×
Anti BCL2-Associated X (Bax)	Abcam, Cambridge, UK	ab32503	1000 ×
Anti B-cell lymphoma-2 (Bcl-2)	Abcam	ab32124	1000 ×
Anti Cleaved Caspase-3	Cell Signaling Technology	9661	1000 ×
Anti fatty acid synthase (FASN)	Cell Signaling Technology	3180	1000 ×
Anti- PI3 Kinase p110 Beta (p-PI3K)	Abcam	ab151549	1000×
Anti phospho-protein kinase B (p-AKT)	Cell Signaling Technology	9271 S	1000×
Anti phospho-mammalian target of rapamycin (anti p-mTOR)	Abcam	ab109268	1000×
Anti β-Actin	Sigma-Aldrich, St. Louis, USA	A3854	50,000×

Animal model and in vivo studies

The animal experiments were conducted at the Southern University of Science and Technology under the approval of the Guangdong Medical Laboratory Animal Center Ethical Committee, with the assigned ethical approval number C202205-24 and D202410-5. BALB/c-nu male mice, 6–8 weeks old, were quarantined in an animal experiment center for 7 days to relieve mental stress. T24 cells were digested and harvested with PBS; the cell density was then adjusted to 0.5×10^5 cells/μL. The mice's skin was carefully sterilized using 75% alcohol solution three times, and then the 80 μL cell suspension mixture was injected subcutaneously into the dorsal region of the mice. After that, all animals were quarantined for another 10–15 days until the tumors became visible to the naked eye. The control group was intraperitoneally injected with 25 μl DMSO once a day. The 3025@ML group was intraperitoneally injected with 25 μl 50 mg/kg 3025@ML once a day. Treatment continued for a total of 30 days. Tumor size was detected using a Vernier caliper, and tumor volume (mm^3) was calculated as $AL \times AW^2 \times 0.52$ [19], where AL and AW refer to the length and width of tumors, respectively. The mice were weighed every three days. To study the tissue distribution of the SRT3025 and OXA after 3025@ML + OXA administration, the subcutaneous tumor model was constructed in 5 nude mice in each group as previously described. The mice were intraperitoneally injected with 50 mg/kg 3025@ML every day and 10 mg/kg OXA once a week. The mice in the control group received the same dose of DMSO solution. After 15 days of administration, the mouse plasma and tissues were collected. Levels of the SRT3025 and OXA were measured by HPLC.

Statistical analysis

The data are presented as means ± SD (error bars) and were analyzed using GraphPad Prism software (Version 8.00). The Mann-Whitney rank sum test was used to evaluate the significant differences with a P value lower than 0.05 was considered significant.

Result

Synthesis and characterization of 3025@ML

The schematic diagram of 3025@ML is shown in Fig. 2A. The diameter of Lipo, Mem, and ML was approximately 100 ~ 200 nm (Fig. 2B), and the zeta potential of ML

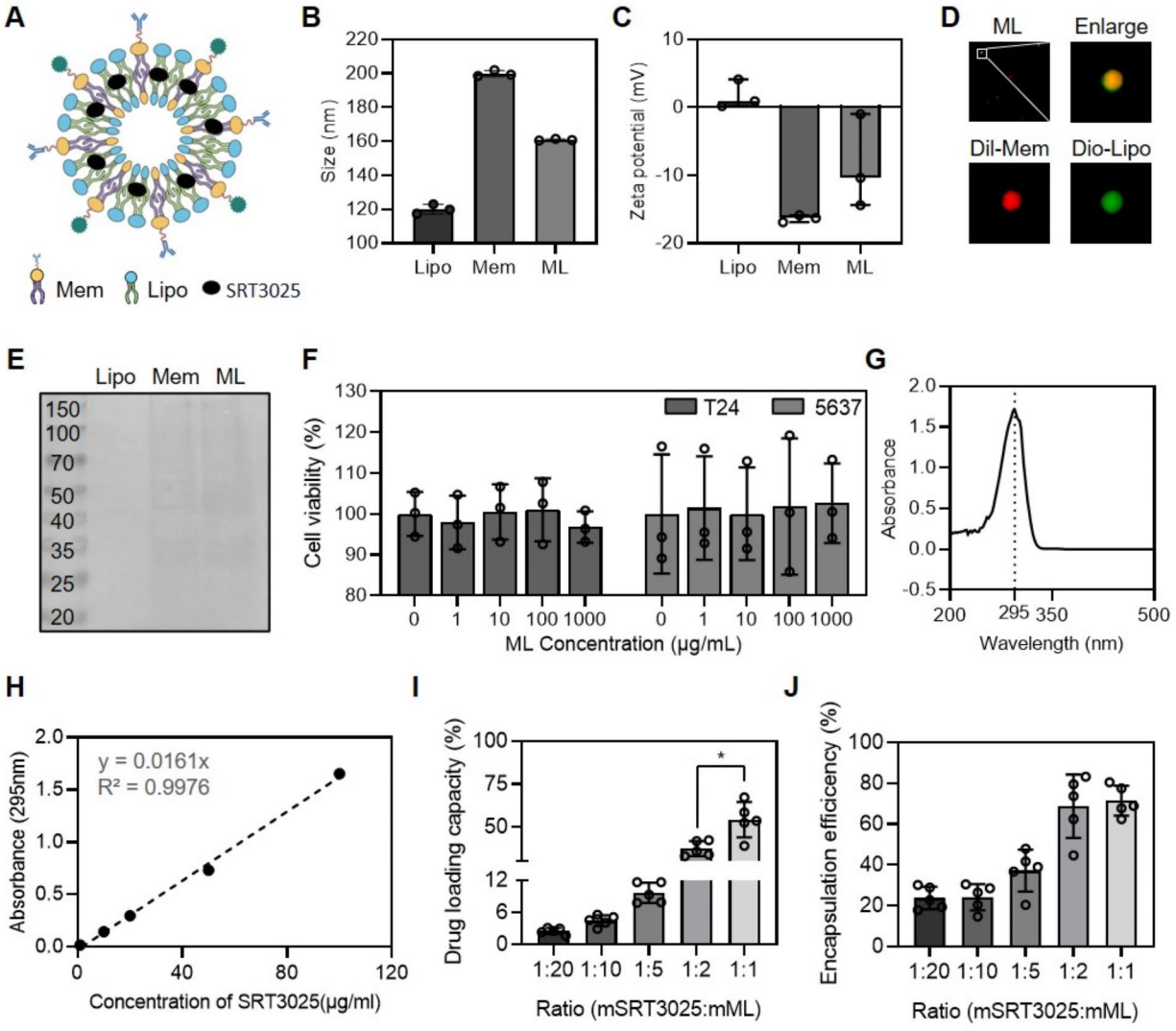

Fig. 2 Synthesis and characterization of 3025@ML. Schematic diagram of 3025@ML (**A**). Diamter (**B**) and zeta potential (**C**) of Lipo, Mem and ML. Fluorescence co-localization (**D**) and western blot (**E**) were used to observe Lipo, Mem, and ML membrane protein expression. CCK8 analysis (**F**) proved that the ML did not affect the proliferation ability of tumor cells. An ultraviolet-visible spectrophotometer detected the maximum absorption wavelength of SRT3025 (**G**). Standard curve of SRT3025 (H). When the mass ratio of SRT3025 to ML was 1:1, 3025@ML had the highest drug loading capacity and high encapsulation efficiency (I and J). Lipo: liposome, Mem: tumor membranes, ML: cell membrane hybrid liposomes. **P*<0.05

was similar to Mem (Fig. 2C). Yellow fluorescent signals produced by the superimposition of red fluorescent Dil-Mem and green fluorescent Dio-Lipo were observed (Fig. 2D). Compared with Lipo, Mem and ML carriers have proteins (Fig. 2E), which indicates that tumor cell membrane-modified liposomes were successfully synthesized.

Different concentrations of ML carriers were used to measure the viability of T24 and 5637 cells by CCK8 assay. It was observed that ML did not markedly affect the growth of tumor cells (Fig. 2F), indicating that ML is biocompatible. The maximum absorption of SRT3025 was detected at a wavelength of 295 nm (Fig. 2G). A standard curve of SRT3025 was prepared using different concentrations of SRT3025 (Fig. 2H). It was observed that 1:1 is the optimal mass ratio of SRT3025 to ML since it has the highest drug loading capacity and high encapsulation efficiency (Fig. 2I and J). According to previous reports, caveolin-1 is known to play critical roles in vesicular endocytosis. The uptake mechanism of these hybrid liposomes in bladder cancer cells was investigated using inhibitors of caveolin-1 (filipin) alongside Dil-labeled 3025@ML via flow cytometry. Results indicated that adding these inhibitors did not affect the cellular uptake efficiency of the liposomes (Figure S1). Based on this, it was hypothesized that the liposome uptake may occur through a simple, energy-independent membrane fusion process.

3025@ML inhibited PKM2 expression and induced cell apoptosis

To determine the effective anti-tumor dose of 3025@ML for in vitro studies, T24 and 5637 cells were treated with 0, 0.1, 1, 10, and 100 μM of 3025@ML for 48 h (Fig. 3A and B). The results showed that 3025@ML significantly reduced the cell viability of both cell types in a dose-dependent manner. To analyze the mechanism of the anti-tumor effect of 3025@ML, bladder cancer cell lines were treated with 3025@ML, and western blot analysis was performed to detect the expression of PKM2 protein and the key proteins of the apoptosis signaling pathway, Bax, Bcl-2, and Cleaved Caspase-3 (Fig. 3C). It was observed that 3025@ML downregulated the expression levels of PKM2 and Bcl-2 and up-regulated the expression of Bax and cleaved caspase-3 in both T24 cells (Fig. 3D) and 5637 cells (Fig. 3E). This suggested that 3025@ML inhibits the expression of PKM2 and induces apoptosis. This indicated that 3025@ML exerts an antitumor effect by inducing apoptosis. 3025@ML significantly decreased the tumor volume and tumor weight, while it did not significantly change the body weight (Fig. 3F and S2).

Compound 3K downregulated PKM2 level to enhance anti-tumor activity of OXA

In order to evaluate the activity of PKM2 in regulating apoptosis, the effect of compound 3K on cell proliferation was determined by using CCK8 to test cell viability. T24 and 5637 cells were treated with different concentrations of compound 3K for 48 h (Fig. 4A). The result showed that compound 3K significantly inhibited the cell viability of T24 and 5637 cells. 10 μM compound 3K + OXA was administered to two bladder cancer cell lines (Fig. 4B and C). Compound 3K significantly increased the chemosensitivity to OXA compared to the two single-drug groups. To examine the relationship between PMK2 and lipid metabolism, PMK2 and FASN were detected by western blot (Fig. 4D and E). This indicates that compound 3K inhibited the expression of PKM2 and FASN and induced cell apoptosis pathway, thereby promoting cell apoptosis.

3025@ML enhanced anti-tumor activity of OXA

To explore whether 3025@ML increases the sensitivity to OXA, T24 and 5637 cell lines were treated with 3025@ML + OXA. CCK8 was used to detect the cell viability, and trypan blue reagent staining was used to detect the cell death rate. The results showed that combined treatment significantly reduced cell viability (Fig. 5A and B) and increased cell death rate (Fig. 5C and D). Flow cytometry analysis showed that 3025@ML + OXA significantly increased the percentage of apoptotic cells in T24 and 5637 cells (Fig. 5E).

To investigate the mechanism of 3025@ML + OXA to promote cell death, a western blot was performed, which showed that the combination of 3025@ML and OXA reduced PKM2 protein expression, thereby reducing FASN protein expression and inhibiting the AKT/mTOR signaling pathway (Fig. 5F and G). The combination of 3025@ML and OXA significantly increased apoptosis in T24 and 5637 cell lines by reducing PKM2 and FASN protein expression and inhibiting the AKT/mTOR signaling pathway (Fig. 6).

To provide insight into its distribution and bioavailability, the levels of 3025@ML in plasma and tissues of BALB/c nude mice are presented in Table S1. RNA sequencing was done to provide complementary insights into the underlying transcriptional changes, furnishing a deeper understanding of the regulatory mechanisms at play. After the cells were treated by 3025@ML, a significant enrichment of genes involved in DNA replication, cell cycle, and apoptosis was observed. Kyoto Encyclopedia of Genes and Genomes analysis demonstrated that 3025@ML regulated the p53 signaling pathway (Figure S3).

Discussion

The present study proved that 3025@ML increased the anti-tumor effect of OXA by impairing the activity of the PI3K/AKT/mTOR signaling pathway and decreasing the expression of PKM2 and FASN. Lipid metabolism has intricate pathways for fatty acid synthesis, oxidation, and lipid transport. Lipids are transported from the liver to peripheral tissues or back to the liver through lipoproteins [20]. It is reported that elevated fatty acid synthesis was observed in several cancer cells resistant to chemotherapy. Wang et al. reported that the receptor of long-chain free fatty acids (FFAs), G protein-coupled receptor 120 (GPR120), was highly expressed in primary breast cancer treated by chemotherapy. The in vitro and in vivo study demonstrated that GPR120 increases the expression of Acetyl-CoA carboxylase, sterol regulatory element-binding transcription factor 1, sterol regulatory element-binding transcription factor 2, and FASN and induces the chemical drugs resistance to breast cancer cells [21]. In the present study, it was also observed that 3025@ML and compound 3K reduced the level of FASN in T24 and 5637 cells and increased the anti-tumor activity of OXA. These findings suggest that targeting FASN is a promising strategy to enhance the therapeutic effect. Although a clinical study demonstrated that omeprazole, a proton pump inhibitor, was tolerable and inhibited the expression of FASN, no study proved that inhibition of FASN significantly prolonged the survival of patients [22]. Therefore, a randomized controlled trial is needed to evaluate the benefits of the combination of chemical drugs and inhibitors of FASN in treating cancer patients.

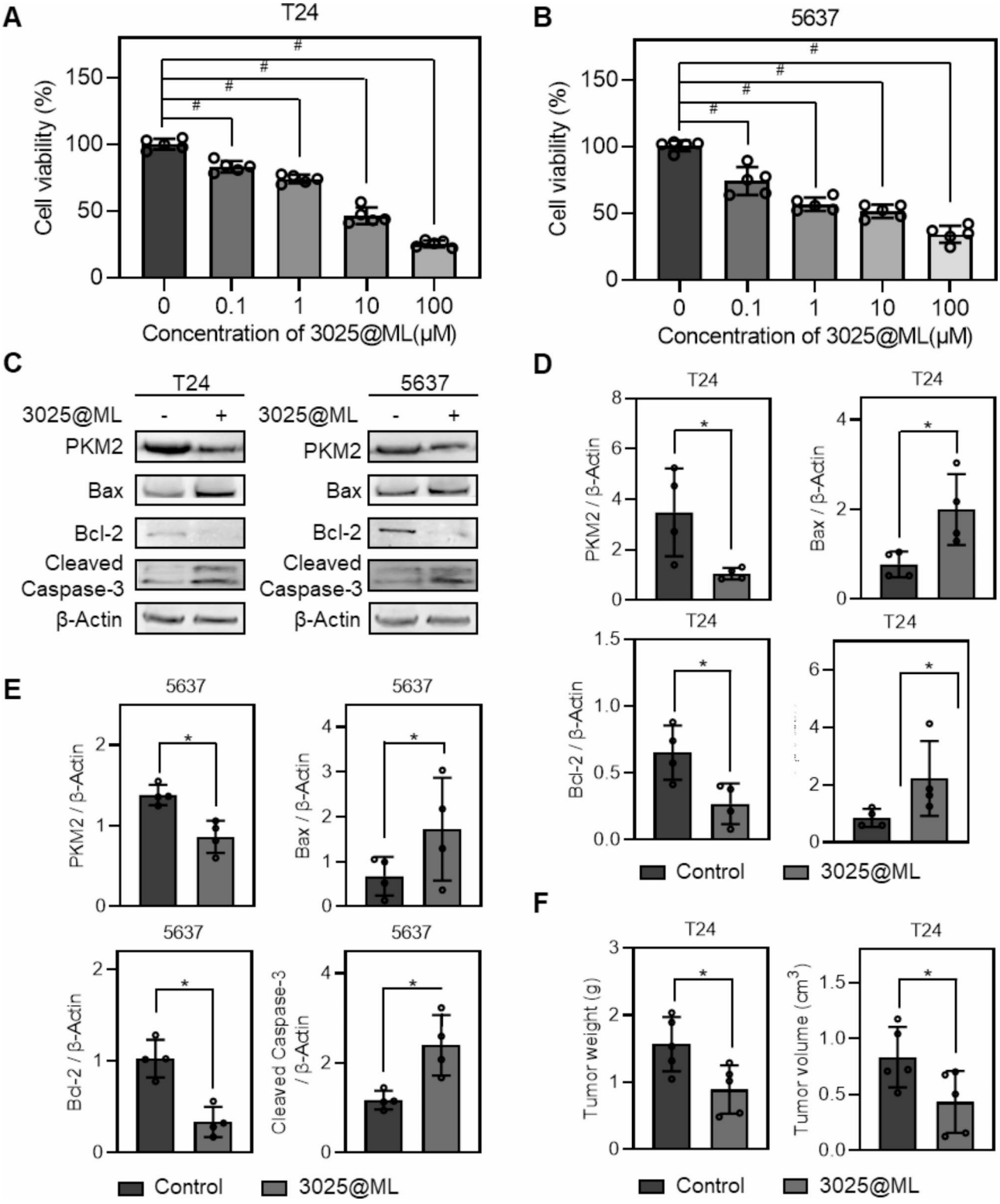

Fig. 3 3025@ML inhibits proliferation and induces cell apoptosis by inhibiting PKM2. (**A** and **B**) CCK8 analysis proved that 3025@ML significantly inhibited the cell viability of T24 cells and 5637 cells. (**C**, **D**, and **E**) Qualitative and quantitative results of Western blot revealed that T24 cells and 5637 cells treated with 3025@ML showed downregulation of PKM2 protein levels and induced apoptosis. (**F**) Tumor weight and Tumor volume. **P*<0.05, #*P*<0.01

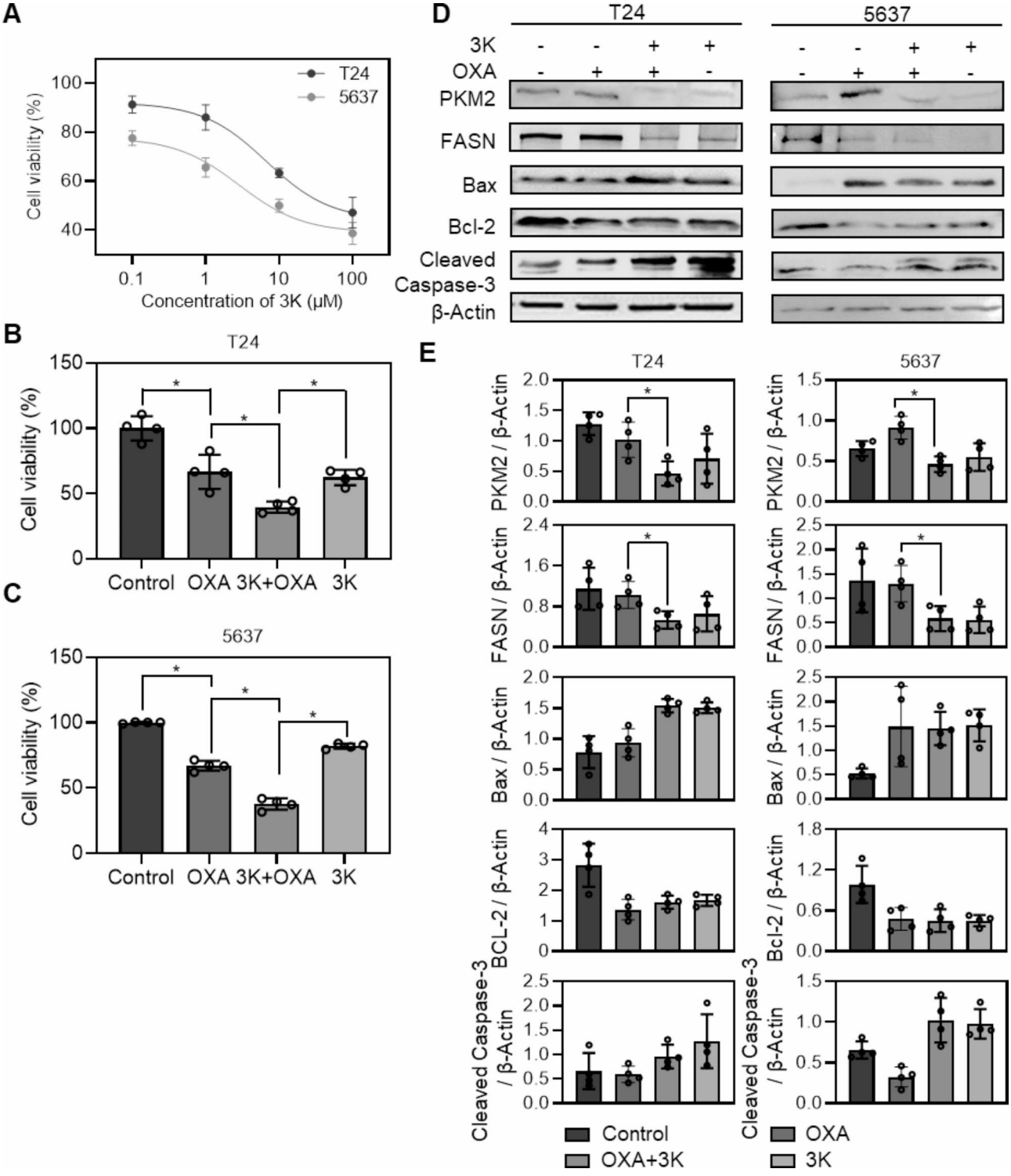

Fig. 4 Compound 3K enhanced the anti-tumor activity of OXA and induced cell apoptosis by inhibiting PKM2 and FASN. CCK8 analysis confirmed that compound 3K inhibited cell viability of T24 cells and 5637 cells (**A**, **B**, and **C**). Compound 3K, OXA, and combination therapy treated T24 cells (**D**) and 5637 cells (**D**). Compound 3K decreased the accumulation of PKM2 and Bcl-2 and increased the expression of Bax and Cleaved Caspase-3. Quantitative analysis of the PKM2, FASN, Bax, Bcl-2, and Cleaved Caspase-3 proteins (**E**). 3K: compound 3K; **P*<0.05

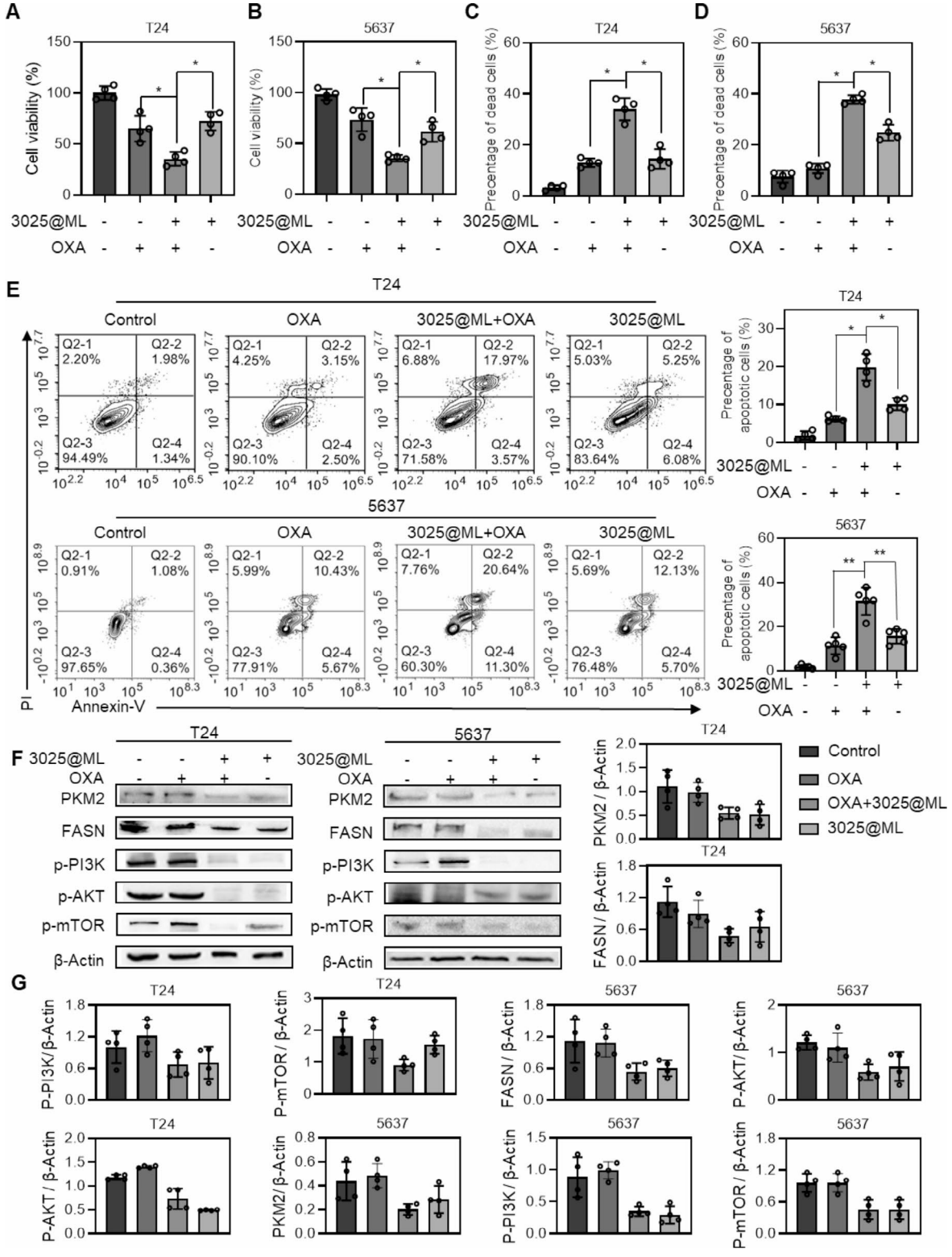

Fig. 5 3025@ML enhanced anti-tumor activity of OXA. T24 cells and 5637 cells were treated with 3025@ML, OXA, or the com by reducing PKM2 and FASN bination to verify 3025@ML enhanced anti-tumor activity of OXA by CCK8 analysis (**A** and **B**) and trypan blue staining (**C** and **D**). This combination therapy significantly reduced cell viability and induced cell death. Annexin V/PI staining (**E**) supported combination therapy enhances the percentage of cell apoptosis. (**F**) Treating the cells with OXA or OXA + 3025@ML caused the downregulation of PKM2, AKT, and mTOR and the decrease of p-AKT and p-mTOR levels. (**G**) Quantitative analysis of the PKM2, FASN, p-AKT, and p-mTOR proteins. **P*<0.05

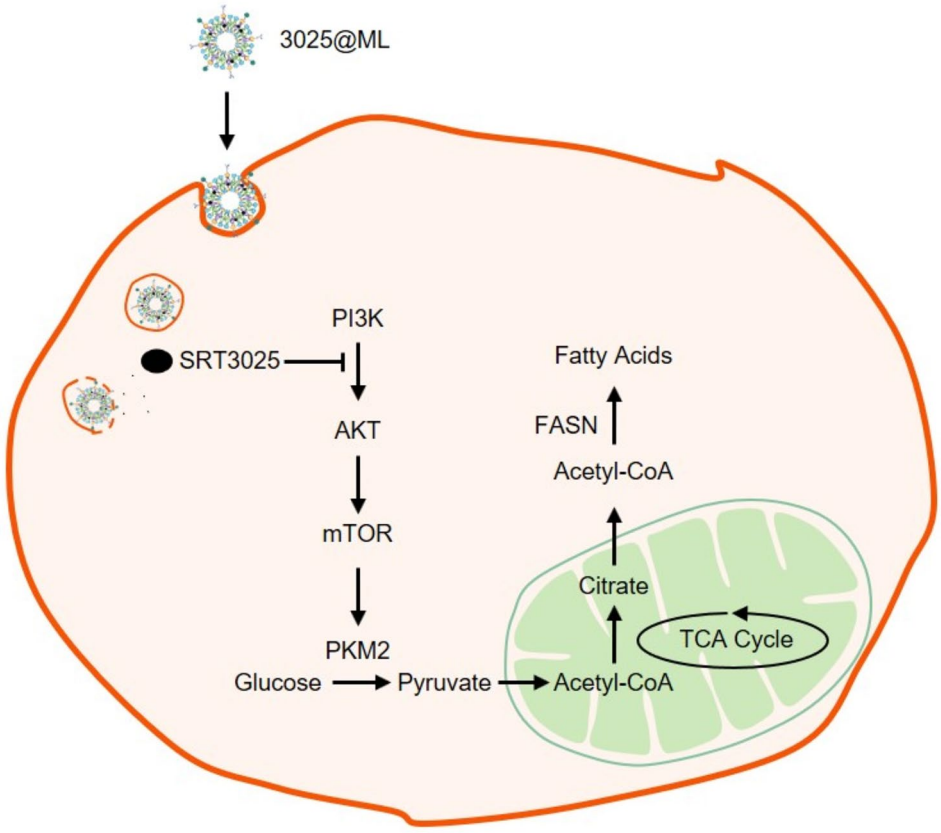

Fig. 6 The anti-tumor activity of 3025@ML via lipid metabolism. PI3K: phosphatidylinositol 3-kinase; AKT: protein kinase B; mTOR: mammalian target of rapamycin; PKM2: pyruvate kinase M2; FASN: fatty acid synthase

Although STACs are considered the activator of the SIRT1 enzyme, numerous studies have proved that the anti-tumor activity of STACs does not rely solely on the activation of SIRT1. For example, Dirk Beher et al. proved that resveratrol, which is claimed to be a traditional SIRT1 activator, failed to acetylate peroxisome proliferator-activated receptor-gamma coactivator-1α (PGC-1α), although SIRT1 deacetylates PGC-1α [23].

In the present study, Western blot analysis proved that 3025@ML enhanced the effect of OXA by inhibiting the activity of PKM2 and FASN. A previous study reported that metformin decreased the accumulation of PKM2 by suppressing the PI3K/AKT/mTOR signaling pathway in esophageal cancer cells [24]; we, therefore, determined the activity of PI3K/AKT/mTOR axis after treating the cells by 3025@ML. The results demonstrated that 3025@ML decreased p-PI3K, p-AKT, p-mTOR, and PKM2 levels. These data also suggested that the level of PKM2 was regulated by the PI3K/AKT/mTOR axis.

3025@ML remarkably enhances the efficacy of OXA by inhibiting key metabolic regulators, particularly PKM2 and FASN. 3025@ML treatment significantly decreased the phosphorylation levels of PI3K, AKT, and mTOR, key components of the PI3K/AKT/mTOR signaling pathway. Notably, the decreased levels of p-PI3K, p-AKT, p-mTOR, and PKM2 suggest a coordinated regulatory mechanism in which 3025@ML reduces PKM2 activity and implicates the PI3K/AKT/mTOR axis (Fig. 6).

The findings show that 3025@ML notably reduced the tumor volume without significant changes in the body weight, presenting strong antitumor activity with a favorable safety profile. Thus, highlighting the potential of 3025@ML as a promising therapeutic option for selective anti-tumor effect. Moreover, the drug's presence in plasma and organs indicates effective systemic distribution, i.e., absorption, metabolism, and circulation, supporting its observed anti-tumor effect. These findings highlight the potential of 3025@ML as a therapeutic agent to modulate metabolic pathways, thus enhancing the anticancer effects of OXA and providing insights into novel therapeutic strategies for tumors.

Strengths

The strength of this study lies in exhibiting that 3025@ML significantly enhanced the anti-cancer effects of OXA by targeting key metabolic modulators, particularly PKM2 and FASN, while also inhibiting the PI3K/AKT/mTOR signaling pathway. It furnishes valuable

mechanistic insights into how 3025@ML modulates lipid metabolism, reduces fatty acid synthesis, and helps overcome compromised therapeutic effects. The combination therapy effectively decreased tumor volume without affecting body weight, exhibiting its potent anti-tumor efficacy and favorable safety profile. Moreover, the systemic distribution of 3025@ML demonstrated its effective absorption, metabolism, and circulation, further supporting its therapeutic potential. These findings highlight the role of 3025@ML in modulating metabolic pathways to improve chemotherapeutic outcomes, offering a promising strategy for enhancing cancer therapy.

Limitations

There are some limitations in the present study. First, although compound 3K and 3025@ML decrease the accumulation of FASN and significantly enhance the anti-tumor activity of OXA, further study still needs to clarify how PKM2 regulates the expression of FASN. This will provide novel regulators of FASN and accelerate the drug development process for bladder cancer. Second, the benefits of 3025@ML in combination with other chemical drugs were not investigated, such as gemcitabine, methotrexate, and docetaxel, which are also used to treat bladder cancer. Future studies also need to evaluate this.

Conclusion

In conclusion, 3025@ML effectively enhances OXA's anti-tumor activity by targeting the PI3K/AKT/mTOR axis to downregulate PKM2 and FASN protein levels. This novel formulation reduces PKM2 and FASN expression, enhancing therapeutic efficacy. The favorable safety profile and systemic distribution exhibit its potential for clinical application, offering a promising strategy for addressing the compromised effect of chemotherapy effect and improving cancer patients' outcomes. In addition, investigating its efficacy in other cancer types and improving the dosing regimen could broaden its clinical application and make it an effective option for personalized cancer therapy. Further studies should, therefore, elucidate the regulatory mechanisms and explore potential synergies with other chemotherapeutic agents for broader clinical applications in cancer treatment.

Abbreviations

OXA	Oxaliplatin
Lipo	Liposome
Mem	Tumor Membrane
ML	The cell Membrane hybrid Liposomes
3025@L	SRT3025-loaded liposomes
3025@ML	SRT3025 loaded cell membrane hybrid liposomes
PKM2	Pyruvate Kinase M2
FASN	Fatty Acid Synthase
STACs	SIRT1-Activating Compounds
Bax	BCL2-Associated X
Bcl-2	B-cell lymphoma-2
PI3K	Phosphatidylinositol 3-kinase
AKT	Protein Kinase B
mTOR	Mammalian target of rapamycin
3K	Compound 3K

Supplementary Information

The online version contains supplementary material available at https://doi.org/10.1186/s12944-025-02431-x.

Supplementary Material 1

Supplementary Material 2

Author contributions

Xiaobin Wang wrote the main manuscript text and supplementary part. Shulin Li and Zichen Li prepared Figs. 1, 2, 3 and 4; Table 1.Zhuona Lin prepared Figs. 5 and 6.Zhifeng Wang revised and improved this article. All authors reviewed the manuscript.

Funding

This study was supported by the Sanming Project of Medicine in Shenzhen Nanshan (SZSM202103003); and Major Scientific and Technological Project of the Health System in Nanshan Shenzhen(NSZD2024062).

Data availability

No datasets were generated or analysed during the current study.

Declarations

Ethical approval

Ethical approval was obtained from the Guangdong Medical Laboratory Animal Center Ethical Committee (Approval number: C202205-24 and D202410-5). All animal procedures were performed in accordance with the relevant ethical guidelines.

Competing interests

The authors declare no competing interests.

Author details

[1]Department of Urology, Southern University of Science and Technology Hospital, Shenzhen 518052, China
[2]Department of Urology, Shenzhen University General Hospital, Shenzhen University, Shenzhen 518055, China
[3]Medical School of Basic Medical Sciences, Shenzhen University, Shenzhen 518060, China
[4]Department of Urology, Henan Provincial People's Hospital, Zhengzhou University People's Hospital, Henan University People's Hospital, Zhengzhou 450003, China

Received: 5 July 2024 / Accepted: 6 January 2025
Published online: 17 January 2025

References

1. Jin YH, Zeng XT, Liu TZ, Bai ZM, Dou ZL, Ding DG, Fan ZL, Han P, Huang YR, Huang X et al. Treatment and surveillance for non-muscle-invasive bladder cancer: a clinical practice guideline (2021 edition). Mil Med Res 2022; 9;44.
2. Anderson RL, Balasas T, Callaghan J, Coombes RC, Evans J, Hall JA, Kinrade S, Jones D, Jones PS, Jones R et al. A framework for the development of effective anti-metastatic agents. Nat Rev Clin Oncol 2019; 16185–204.
3. Yang X, Zhang S, Cui Y, Li Y, Song X, Pang J. Efficacy and safety of transurethral resection of bladder tumour combined with chemotherapy and immunotherapy in bladder-sparing therapy in patients with T1 high-grade or T2 bladder cancer: a protocol for a randomized controlled trial. BMC Cancer 2023; 23;320.
4. Zhang Y, Chen X, Lin J, Jin X. Biological functions and clinical significance of long noncoding RNAs in bladder cancer. Cell Death Discov. 2021;7:278.
5. Linares J, Sallent-Aragay A, Badia-Ramentol J, Recort-Bascuas A, Méndez A, Manero-Rupérez N, Re DL, Rivas EI, Guiu M, Zwick M et al. Long-term

platinum-based drug accumulation in cancer-associated fibroblasts promotes colorectal cancer progression and resistance to therapy. Nat Commun 2023; 14;746.
6. Jin H, He Y, Zhao P, Hu Y, Tao J, Chen J, Huang Y. Targeting lipid metabolism to overcome EMT-associated drug resistance via integrin β3/FAK pathway and tumor-associated macrophage repolarization using legumain-activatable delivery. Theranostics 2019; 9;265–278.
7. Xia Y, Sun M, Huang H, Jin WL. Drug repurposing for cancer therapy. Signal Transduct Target Ther. 2024;9:92.
8. Wang Y, Hao F, Nan Y, Qu L, Na W, Jia C, Chen X. PKM2 inhibitor shikonin overcomes the cisplatin resistance in bladder Cancer by inducing necroptosis. Int J Biol Sci. 2018;14:1883–91.
9. Pandkar MR, Sinha S, Samaiya A, Shukla S. Oncometabolite lactate enhances breast cancer progression by orchestrating histone lactylation-dependent c-Myc expression. Transl Oncol. 2023;37:101758.
10. Li YQ, Sun FZ, Li CX, Mo HN, Zhou YT, Lv D, Zhai JT, Qian HL, Ma F. RARRES2 regulates lipid metabolic reprogramming to mediate the development of brain metastasis in triple negative breast cancer. Mil Med Res. 2023;10:34.
11. Luo P, Zhang Q, Zhong TY, Chen JY, Zhang JZ, Tian Y, Zheng LH, Yang F, Dai LY, Zou C et al. Celastrol mitigates inflammation in sepsis by inhibiting the PKM2-dependent Warburg effect. Mil Med Res 2022; 9;22.
12. Wong N, De Melo J, Tang D. PKM2, a Central Point of Regulation in Cancer Metabolism. Int J Cell Biol 2013; 2013;242513.
13. Ginés A, Bystrup S, Ruiz de Porras V, Guardia C, Musulén E, Martínez-Cardús A, Manzano JL, Layos L, Abad A, Martínez-Balibrea E. PKM2 subcellular localization is involved in Oxaliplatin Resistance Acquisition in HT29 Human Colorectal Cancer Cell lines. PLoS ONE 2015; 10e0123830.
14. Chini CC, Espindola-Netto JM, Mondal G, Guerrico AM, Nin V, Escande C, Sola-Penna M, Zhang JS, Billadeau DD, Chini EN. SIRT1-Activating compounds (STAC) negatively regulate pancreatic Cancer cell growth and viability through a SIRT1 lysosomal-dependent pathway. Clin Cancer Res 2016; 222496–2507.
15. Zhao S, Sun Y, Wu X, Yang Y, Fan K, Hu K, Qin Y, Li K, Lin L, Chen K et al. Sirtuin 1 activator alleviated lethal inflammatory injury via promotion of autophagic degradation of pyruvate kinase M2. Front Pharmacol 2023; 14;1092943.
16. He B, Sui X, Yu B, Wang S, Shen Y, Cong H. Recent advances in drug delivery systems for enhancing drug penetration into tumors. Drug Deliv 2020; 271474–1490.
17. Zhang W, Fan Y, Zhang J, Shi D, Yuan J, Ashrafizadeh M, Li W, Hu M, Abd El-Aty AM, Hacimuftuoglu A et al. Cell membrane-camouflaged bufalin targets NOD2 and overcomes multidrug resistance in pancreatic cancer. Drug Resist Updat 2023; 71;101005.
18. Zhang W, Chen L, Cui M, Xie L, Xi Z, Wang Y, Shen X, Xu L. Successively triggered rod-shaped protocells for enhanced tumor chemo-photothermal therapy. Eur J Pharm Biopharm. 2021;169:1–11.
19. Tomayko MM, Reynolds CP. Determination of subcutaneous tumor size in athymic (nude) mice. Cancer Chemother Pharmacol 1989; 24;148–154.
20. Liu Q, Zhang X, Qi J, Tian X, Dovjak E, Zhang J, Du H, Zhang N, Zhao J, Zhang Y et al. Comprehensive profiling of lipid metabolic reprogramming expands precision medicine for HCC. Hepatology : 2024.
21. Wang X, He S, Gu Y, Wang Q, Chu X, Jin M, Xu L, Wu Q, Zhou Q, Wang B, et al. Fatty acid receptor GPR120 promotes breast cancer chemoresistance by upregulating ABC transporters expression and fatty acid synthesis. EBioMedicine. 2019;40:251–62.
22. Sardesai SD, Thomas A, Gallagher C, Lynce F, Ottaviano YL, Ballinger TJ, Schneider BP, Storniolo AM, Bauchle A, Althouse SK et al. Inhibiting fatty acid synthase with omeprazole to improve efficacy of Neoadjuvant Chemotherapy in patients with operable TNBC. Clin Cancer Res 2021; 275810–5817.
23. Beher D, Wu J, Cumine S, Kim KW, Lu SC, Atangan L, Wang M. Resveratrol is not a direct activator of SIRT1 enzyme activity. Chem Biol Drug Des 2009; 74;619–624.
24. Tang JC, An R, Jiang YQ, Yang J. Effects and mechanisms of Metformin on the proliferation of Esophageal Cancer cells in Vitro and in vivo. Cancer Res Treat 2017; 49778–789.

Publisher's note